Hindawi
Advances in Civil Engineering
Volume 2024, Article ID 5594519, 6 pages
https://doi.org/10.1155/2024/5594519

Research Article

Reverse Model for Curved Bridge Measurement Based on 3D Laser Scanning Technology

Xin Chen,[1] **Lihang Chen**,[2] **and Dong Liang**[2]

[1]*Hebei Expressway Group Limited, Huailai, Hebei, China*
[2]*School of Civil and Transportation Engineering, Hebei University of Technology, Tianjin, China*

Correspondence should be addressed to Lihang Chen; 202111601012@stu.hebut.edu.cn

Received 25 August 2023; Revised 26 February 2024; Accepted 18 March 2024; Published 3 April 2024

Academic Editor: Krishanu Roy

Receiving inspection plays a crucial role in ensuring construction quality after the completion of engineering projects. Traditional inspection measurement methods, such as manual observation means and optical equipment measurement methods, have limitations in terms of the number of measurement sites and the range of measurements. These traditional methods fail to provide accurate curve parameters and continuous spatial morphology information for large-span curved bridge structures. This paper proposes a reverse model measurement method to address this issue. The reverse model is built based on point cloud data acquired by 3D laser scanning technology. Finally, take the Taizicheng No. 1 Bridge as an example, the validity of the proposed method is verified.

1. Introduction

Bridge engineering is currently undergoing significant advancements due to the increasing number of infrastructure projects involving river and sea crossings. Bridge construction evolves with longer spans, more complex shapes, innovative structural designs, and advanced construction techniques [1]. Therefore, large-span curved bridge structures are most chosen although there are more restrictive requirements that need to be considered in the design of curved bridges, such as bending moment, torque, combined bending and torsion, and more complex forces, compared with the small-span and linear ones [2].

For large-span curved bridge structures, the inspection of their accurate curve parameters and continuous spatial morphology information is the most difficult problem [3–5]. Traditional inspection measurement methods are manual observation means and optical equipment measurement methods including total stations, theodolite instruments, and laser range finders, and they are generally used to measure linear parameters. The manual observation measurement is always limited by various adverse environmental conditions such as large spans and the high height of bridges, not to mention the disadvantages of being error-prone. The optical equipment measurement methods, such as surveying and mapping with total stations [6], have obvious shortcomings of finite and discrete measurement sites and limited measurement range. So they fail to provide accurate curve parameters and continuous spatial morphology information for large-span curved bridge structures. Therefore, a measurement method for acquiring accurate curve parameters and continuous spatial morphology information for large-span curved bridge structures is urgently needed.

3D laser scanning technology, as a real scene replication technology, is rapidly developing and is increasingly adopted in measurement because it is fast and accurate in data acquisition and can extract comprehensive spatial morphology information for structural analysis and calculation [7]. It has been widely used in the measurement of ancient Chinese wooden structure buildings [8], the safety assessment of pedestrian bridges [9], the displacement changes of a bridge during the construction phase by analyzing the 3D point cloud dataset scanned several times [10], and the damage's extent prediction of bridges [11]. It has also been used effectively in bridge construction and maintenance [12] and deformation monitoring of large-span steel structures [13]. The 3D laser scanning technology can comprehensively obtain precise geometry parameter information and has reached a millimeter level, satisfying the need to comprehensively obtain the

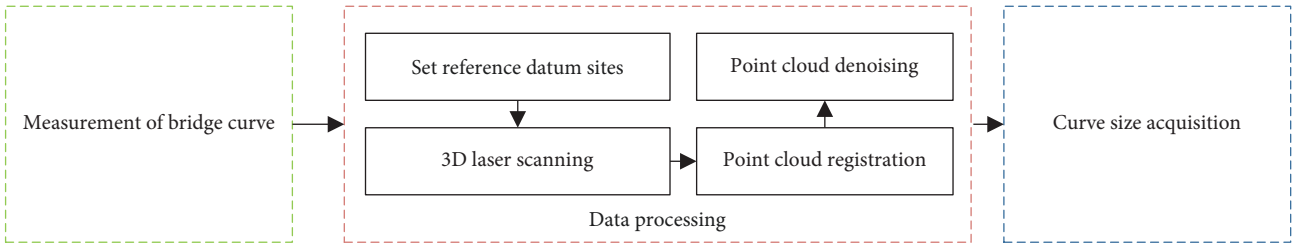

Figure 1: The diagram of procedures.

Table 1: The parameters of Scan Station P40.

Parameter	Distance accuracy	Scanning rate	Point accuracy	Target acquisition accuracy	Scanning range
Data	1.2 mm + 10 ppm	1 million points/s	3 mm @ 50 m; 6 mm @ 100 m	2 mm @ 50 m	360° horizontally; 290° vertically

spatial geometry information of complex-shaped curved bridge structures. However, it is only used for the linear dimension measurement of small structures, not yet in the curve parameter measurement for large-span curved bridge structures.

In this paper, the reverse models of large-span curved bridges are established based on 3D laser scanning technology to obtain accurate curve parameters and continuous spatial morphology information. The main processes are divided into three steps as follows. First, the point cloud data of large-span curved bridges is obtained through 3D laser scanning technology; second, the reverse models, namely the continuous spatial morphology information, of the bridges are obtained after the point cloud data are processed by specific processing algorithms; and third, using the reverse model, the curve parameters of large-span curved bridges can be calculated accurately. The diagram of procedures is shown in Figure 1.

2. Data Processing Methodology

The laser signal is transmitted by a laser pulse transmitter, which is inside a 3D laser scanner, to the surface of a target object. After arriving at the surface, it will return to the receiver along the original path, so the point cloud of the surface can be obtained. In this paper, a 3D laser scanner named Scan Station P40 was used, the exact parameters of which are shown in Table 1.

2.1. Set Reference Datum Sites. Due to the large span of bridges, multiple scans are required to obtain the overall point cloud data of the bridges. The coordinates of each scanned point cloud exist in different coordinate systems, so they must be unified into one same coordinate system so that the overall point cloud model of the target subject can be obtained. For this point, a global positioning system (GPS) control network method is adopted to solve this problem. The GPS is a satellite-based navigation system that provides accurate positioning, usually expressed in terms of longitude, latitude, and altitude, of any point on Earth. A GPS control network method is used to set reference sites accurately. These reference sites are important to unify all point clouds of different coordinate systems into one same coordinate system.

There are two requirements for reference site setting [14]. One is that there should be no obstruction for GPS to receive satellite signals. The other one is that the site should be as far away from the transmission line as possible to avoid the interference of other electromagnetic signals to the satellite signal.

2.2. 3D Laser Scanning. After setting reference sites, 3D laser scanning work can be carried out. The scanning sites of 3D laser scanners are determined according to the actual situation. Increasing the number of scanning sites is necessary if there are many obscures around the target object. Otherwise, the overall structure data of the target object cannot be obtained completely. At least two reference datum sites must be laid out between adjacent scanning stations for subsequent point cloud registration.

2.3. Point Cloud Registration. The essence of point cloud registration is to transform all point clouds scanned from each scanning site into one same coordinate system, so the point cloud reverse model of the target object can be obtained after point cloud registration. Reference sites set by the GPS control network method are extremely important references during the point cloud registration process. Through the spatial coordinates of reference sites, the overall point cloud registration of the object can be realized. Take the registration process of adjacent two sets of point clouds as an example. Their coordinates belong to two different coordinate systems because they are scanned from different scanning sites. The Procrustes analysis technique [15] is adopted to unify these coordinates into one coordinate system, which is often used to deal with two sets of data that have a similar structure but may have different rotations, and translations, namely, in different coordinate systems. Given that the same reference site exists in two adjacent groups of point clouds, it is possible to unify the coordinates into one coordinate system if the transformation relationships, rotation matrices, and translation matrices between them can be calculated.

The singular value decomposition [16] is the one to figure out the rotation matrix R and translation matrix T between two sets of point cloud coordinates. Then, two sets of point clouds can be unified into one same unified coordinate system through Equation (1):

$$A = BR + T + E, \tag{1}$$

where matrix A and matrix B are the representations of two sets of point cloud coordinates, respectively. The matrix E is the error matrix after conversion between matrix A and matrix B.

2.4. Point Cloud Denoising. The scanning rate of the Scan Station P40 is 1 million points/s, so plenty of point clouds will be obtained after the whole scanning operation. During the scanning process, many duplicate and useless point clouds, from something around the target object, will inevitably be obtained due to some unpredictable factors such as instrument error or improper manual operation. These point clouds will have an adverse impact on later data processing, so they must be deleted.

The mean shift algorithm is a density-based algorithm that can discover clusters of arbitrary shapes in multidimensional space [17, 18] and is widely used in image processing, computer vision, and data analysis. Its computational process refers to iteratively moving the core toward the highest density. It is achieved by calculating the mean value of the points within a given radius and moving the core toward the mean, which continues until convergence, i.e., until the core no longer moves significantly. The calculation steps are as follows. First, calculate the offset of the current point to the mean point and move the current point to its offset mean. Then, use it as a new starting point and continue to move until the set threshold is met. Through the iterative process of the mean shift algorithm, each point cloud can be moved to the maximum probability position on the surface of the point cloud model, which means that the noise reduction process of the point cloud model is completed. This algorithm can effectively filter out duplicate and useless point clouds [19], so it is adopted for point cloud denoising.

3. Case Study

3.1. Bridge Overview. The Yanqing–Chongli Expressway, or the Yanchong Expressway for short, is a liaison road between the 2019 World Expo Park Road and the 2022 Winter Olympic Games venue. Taizicheng Bridge is an important bridge in the Hebei section of the Yan Chong Expressway. Taizicheng No. 1 Bridge is in Zhangjiakou City and is part of the Taizi Cheng Interchange. The first right-hand section of it is a cable-stayed bridge with a double-tower and double-cable deck steel box girder, the span arrangement of which is 25 + 60 + 120 + 60 m. The rendering of the Taizicheng No. 1 Bridge is shown in Figure 2. Due to the large-span curved bridge structures, the reverse model measurement method is applied to measure its curve parameters and continuous spatial morphology information for receiving inspection.

Figure 2: Taizicheng No. 1 Bridge.

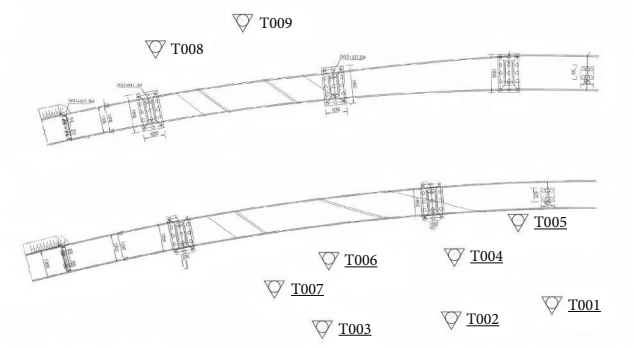

Figure 3: Reference sites.

3.2. Reference Site Setting. According to the complex characteristics of the bridge, nine scanning sites are named from T001 to T009 separately and placed around the bridge, as shown in Figure 3. T001, T002, and T003 are laid on the nearby half-hillside, and the remaining six sites are located on the east side of the right bridge and the west side of the left bridge.

3.3. 3D Laser Scanning Setting. The scanning accuracy of the laser scanner is 3 mm @ 50 m. However, during the measurement process on-site, to ensure higher accuracy, the distance between the location of the measuring point and the target object is generally controlled between 10 and 20 m. With such scanning accuracy, it is possible to obtain sufficiently accurate point clouds and reduce operation time. For structures such as piers, fabrications, and towers, increase the number of scans and reduce the distance between two adjacent scanning stations so that the point clouds of local details structures can be obtained.

3.4. Point Cloud Registration. Import the scanned point cloud data and the spatial coordinates of reference sites into the Cyclone software, a specialized data processing software. Transform the coordinates of all point clouds into the same coordinate system using point cloud registration between two adjacent scanning stations. The reverse model of the large-span curved bridge is obtained in digital form, the result of which is shown in Figure 4.

3.5. Point Cloud Denoising. The mean drift algorithm is used for point cloud denoising. Input initialized original point clouds. Set the value domain window width $hr \leq 0$ and the

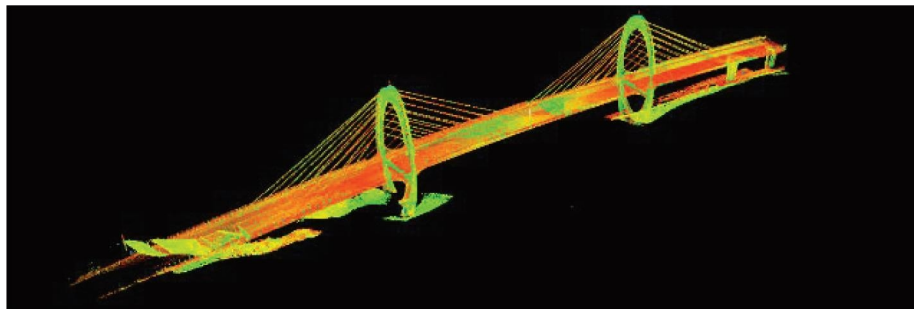

Figure 4: The point cloud of the whole bridge.

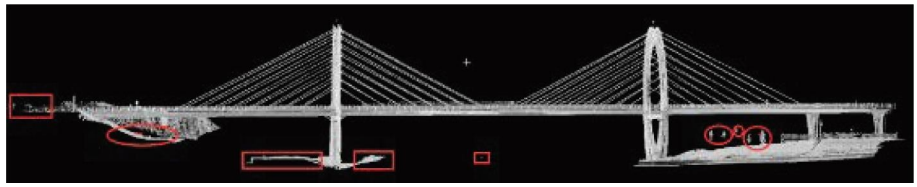

Figure 5: Original point clouds.

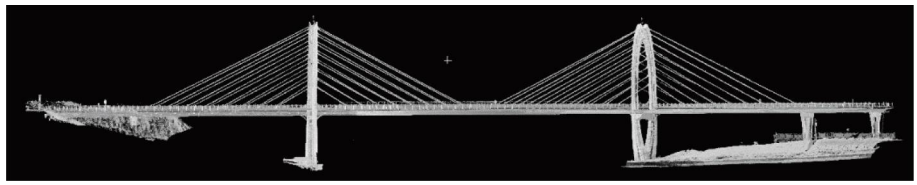

Figure 6: Point clouds after drift algorithm processing.

null domain window width $hs \leq 0$. Make $\varepsilon = 2 \times hs$, then calculate the Gaussian kernel function which is shown in Equation (2):

$$G = \exp(-G.hs/hs). \quad (2)$$

After iterative calculation, the smoothed point clouds can be obtained. A comparison of original point clouds and ones after denoising is shown in Figures 5 and 6. From the comparison of the two figures, we can see that the duplicate and useless point clouds caused by external environmental factors such as vibration, temperature, wind, dust, etc., have been filtered.

4. Bridge Curve Parameter

The curve radius of the bridge is 1,100 m. The traditional method is not practical and accurate for curve parameter acquisition because it can only select a few points to reflect the overall configuration of the bridge.

4.1. Curve Parameter Acquisition Methodology. Using the reverse model, the curve parameter of the large-span curved bridge can be calculated accurately. The calculation processes are divided into three steps. First, project the bridge according to the actual situation. The Taizicheng No. 1 Bridge studied in this paper is in the north–south direction, so the fitting of the bridge curve radius is projected to the XOY plane; second, extract representative point clouds of bridge curves. The Levenberg–Marquardt algorithm [16] is used to extract point cloud data of the curved shape of the bridge, which can provide numerical solutions for nonlinear minimization. This algorithm can combine the advantages of the Gauss–Newton algorithm and the gradient descent method by modifying the parameters during execution. After several iterations, representative points of bridge curves are obtained. Third, fit the projected 2D points. Since the bridge is a curved bridge with a constant curvature, the circular function is directly used to fit the projected points of the XOY plane of the bridge. It should be pointed out that when the fitting analysis is performed, reasonable functions are adopted to perform according to specific bridge geometric features, otherwise the obtained fitting equation is meaningless.

4.2. Analysis of Fitting Curve. The fitting equation of the curve radius is shown in Equation (3). R-squared, a commonly used statistic, is the coefficient of determination and is used to measure how well a statistical model fits the observed data. R-square values range from 0 to 1, with values closer to 1 indicating that the model fits the data better. The fitting result of Equation (3) is 0.99997, the curve fitting result of which is shown in Figure 7. The error of the curve radius between the design value and the calculated one is 0.17%, indicating that the calculation result is accurate:

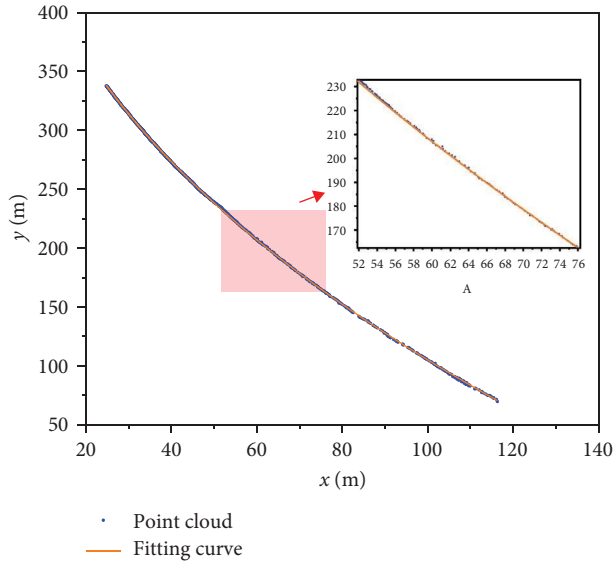

Figure 7: The fitting curve of curve radius.

$$(x - 1{,}101.95)^2 + (y - 557.24)^2 = 1{,}099.22^2. \quad (3)$$

5. Discussion

Regarding the comparison between the traditional measurement methods and the proposed method in this paper. Traditional methods are only suitable for measuring the linear parameters of small-scale components. During the measurement process, several factors will affect the accuracy of measurement results, including the selection of different measurement locations, manual operation errors, and calculation errors. Therefore, they are not suitable for measuring the curve parameters of curved components, not to mention for large-span curved bridge structures. In contrast, the proposed method can completely obtain the continuous spatial morphology information and accurately calculate the curve parameters of large-span curved bridge structures. Although the efficiency of the reverse model method, including scanning time and data processing time, is roughly the same as that of traditional measurement methods, the practicability and accuracy of the proposed method are undoubtedly better.

6. Conclusion

This study focuses on accurately measuring the curve parameter of large-span and complex curved bridges after on-site construction. By utilizing 3D laser scanning technology and reverse model measurement, the previous challenge of accurately measuring the curve parameter of curved bridges has been addressed. The approach was successfully implemented during the receiving inspection of the Taizicheng No. 1 Bridge, with the geometric features of curved bridges being fitted using 3D laser scanning technology and reverse modeling. The error between the design value of the curve radius and the fitted value was found to be 0.17%, indicating a good fitting effect. This study presents a practical and reasonable method for measuring the curve parameter of curved bridges, which could potentially be widely adopted in the receiving inspection of large-scale curved structures in the future. Future research could focus on the real-time monitoring of bridges using 3D laser scanning technology.

Data Availability

The data used to support the findings of this study are included in this paper.

Disclosure

Our research does not involve human participants and animals.

Conflicts of Interest

The authors declare that they have no conflicts of interest.

Acknowledgments

The work was supported by the National Natural Science Foundation of China (No. 51978236).

References

[1] X. Zhou and X. Zhang, "Thoughts on the development of bridge technology in China," *Engineering*, vol. 5, no. 6, pp. 1120–1130, 2019.

[2] Z. Fang, D. Jiechao, Z. Kaiquan, Y. Qian, and Q. Youjiu, "State-of-the-art review of planning and protection of bridge cultural heritage in 2020," *Journal of Civil and Environmental Engineering*, vol. 43, pp. 252–260, 2021.

[3] R. E. Philip, A. D. Andrushia, A. Nammalvar, B. G. A. Gurupatham, and K. Roy, "A comparative study on crack detection in concrete walls using transfer learning techniques," *Journal of Composites Science*, vol. 7, no. 4, Article ID 169, 2023.

[4] G. Beulah Gnana Ananthi, K. Roy, A. M. M. Ahmed, and J. B. P. Lim, "Non-linear behaviour and design of web stiffened battened built-up stainless steel channel sections under axial compression," *Structures*, vol. 30, pp. 477–494, 2021.

[5] B. G. A. Gurupatham, K. Roy, G. M. Raftery, and J. B. P. Lim, "Influence of intermediate stiffeners on axial capacity of thin-walled built-up open and closed channel section columns," *Buildings*, vol. 12, no. 8, Article ID 1071, 2022.

[6] J. P. Delgado, P. R. Soria, B. C. Arrue, and A. Ollero, "Bridge mapping for inspection using an UAV assisted by a total station," in *ROBOT 2017: Third Iberian Robotics Conference*, vol. 2, pp. 309–319, Springer, Cham, 2018.

[7] Y. Wang, Q. Chen, Q. Zhu, L. Liu, C. Li, and D. Zheng, "A survey of mobile laser scanning applications and key techniques over urban areas," *Remote Sensing*, vol. 11, no. 13, Article ID 1540, 2019.

[8] L. Ke, "Application of 3d laser geometry acquiring based on the requirement of ancient architecture conservation and renovation," Beijing, 2019.

[9] L. Dong, Z. Shuo, and Z. Kai, "A 3d laser scanning method for detecting overall configuration of a pedestrian bridg," *Journal of Highway and Transportation Research and Development*, vol. 37, no. 9, pp. 57–66, 2020.

[10] "Spatial change tracking of structural elements of a girder bridge under construction using 3D point cloud," in *ASCE International Conference on Computing in Civil Engineering 2019*, American Society of Civil Engineers, Reston, VA, 2019.
[11] S.-E. Chen, W. Liu, H. Bian, and B. Smith, "3D LiDAR scans for bridge damage evaluations," in *Forensic Engineering 2012: Gateway to a Safer Tomorrow*, pp. 487–495, 2013.
[12] D. Kim, Y. Kwak, and H. Sohn, "Accelerated cable-stayed bridge construction using terrestrial laser scanning," *Automation in Construction*, vol. 117, Article ID 103269, 2020.
[13] M. Guo, M. Sun, D. Pan et al., "High- precision detection method for large and complex steel structures based on global registration algorithm and automatic point cloud generation," *Measurement*, vol. 172, Article ID 108765, 2021.
[14] P. K. Enge, "The global positioning system: signals, measurements, and performance," *International Journal of Wireless Information Networks*, vol. 1, pp. 83–105, 1994.
[15] F. Case, A. Beinat, F. Crosilla, and I. M. Alba, "Virtual trial assembly of a complex steel structure by generalized procrustes analysis techniques," *Automation in Construction*, vol. 37, pp. 155–165, 2014.
[16] K. Baker, "Singular value decomposition tutorial," *The Ohio State University*, vol. 24, 2005.
[17] K. L. Wu and M. S. Yang, "Mean shift-based clustering," *Pattern Recognition*, vol. 40, no. 11, pp. 3035–3052, 2007.
[18] D. Demirović, "An implementation of the mean shift algorithm," *Image Processing on Line*, vol. 9, pp. 251–268, 2019.
[19] H. Liangliang, W. Renhuang, and L. Yongxiogn, "Study on the denoising method of extracting feather rods based on the mean drift," *Automation & Information Engineering*, vol. 36, no. 1, pp. 41–43, 2015.